HHS Public Access

Author manuscript

Xenobiotica. Author manuscript; available in PMC 2019 March 01.

Published in final edited form as:

Xenobiotica. 2018 March ; 48(3): 219–231. doi:10.1080/00498254.2017.1296208.

A novel in vitro allometric scaling methodology for aldehyde oxidase substrates to enable selection of appropriate species for traditional allometry

Rachel D. Crouch[1], **J. Matthew Hutzler**[2], and **J. Scott Daniels**[1]

[1] Department of Pharmacology, Vanderbilt University School of Medicine, Nashville, Tennessee, U.S.A.

[2] Q[2] Solutions, Bioanalytical and ADME Labs, Indianapolis, Indiana, U.S.A.

Abstract

1. Failure to predict human pharmacokinetics of aldehyde oxidase (AO) substrates using traditional allometry has been attributed to species differences in AO metabolism.

2. To identify appropriate species for predicting human *in vivo* clearance by single species scaling (SSS) or multispecies allometry (MA), we scaled *in vitro* intrinsic clearance (CL_{int}) of five AO substrates obtained from hepatic S9 of mouse, rat, guinea pig, monkey, and minipig to human *in vitro* CL_{int}.

3. When predicting human *in vitro* CL_{int}, average absolute fold-error was ≤ 2.0 by SSS with monkey, minipig, and guinea pig (rat/mouse >3.0), and was <3.0 by most MA species combinations (including rat/mouse combinations).

4. Interspecies variables, including fraction metabolized by AO ($F_{m,AO}$) and hepatic extraction ratios (E) were estimated *in vitro*. SSS prediction fold-errors correlated with the animal:human ratio of E (r^2 =0.6488), but not $F_{m,AO}$ (r^2 =0.0051).

5. Using plasma clearance (CL_p) from the literature, SSS with monkey was superior to rat or mouse at predicting human CL_p of BIBX1382 and zoniporide, consistent with *in vitro* SSS assessments.

6. Evaluation of *in vitro* allometry, $F_{m,AO}$, and E, may prove useful to guide selection of suitable species for traditional allometry and prediction of human pharmacokinetics of AO substrates.

Keywords

aldehyde oxidase; clearance; S9; molybdenum hydroxylase; pharmacokinetics; non-cytochrome P450; drug metabolism; species differences

Address correspondence to: J. Scott Daniels, Ph.D., Sano Informed Prescribing, Inc. 393 Nichol Mill Lane, Franklin, TN 37067. scott@thinksano.com.

Declaration of Interest

The authors report no conflicts of interest. The authors are responsible for the content and writing of the article.

Introduction

Aldehyde oxidase (AO) is a molybdo-flavoenzyme known to oxidize aldehydes and aromatic azaheterocycles, as well as reduce N- or S-oxides, nitro groups and some heterocycles. Interest in AO-mediated drug metabolism has increased in recent years as new generations of drug candidates increasingly contain AO-susceptible aromatic azaheterocyles (Pryde *et al.*, 2010). Moreover, the termination of several promising development programs during clinical trial assessment due to unrecognized or underestimated AO metabolism highlights the necessity for innovative approaches to predict human pharmacokinetics (PK) and disposition where AO is the primary clearance mechanism. For example, discontinuation of BIBX1382 (Dittrich *et al.*, 2002), FK3453 (Akabane *et al.*, 2011), and RO1 (Zhang *et al.*, 2011) during clinical trials resulted from unexpectedly poor oral bioavailability attributed to AO-mediated clearance that went unidentified in preclinical and *in vitro* studies. The use of microsomes (lacking cytosol, thus lacking AO) and preclinical species with decreased AO activity (e.g. rat), or in species altogether missing an AO metabolism gene (e.g. dog), ultimately resulted in a lack of clinical translation in PK and anticipated exposure of these candidate drugs (and their metabolites).

A challenge in predicting human drug disposition where AO-mediated metabolism predominates has been attributed to species differences in AO expression and activity. While humans express only one functional gene, *AOX1*, AO expression in other species commonly used to model human PK ranges anywhere from 2–4 isoforms (e.g. rat) to a complete absence of the gene in dog (dog does express non-hepatic, non-drug metabolizing isoforms) (Garattini and Terao, 2012). Human liver S9, cytosolic fractions, and hepatocytes have proven useful in identifying AO metabolism, although at times these systems have resulted in under-prediction or variable activity, proposed to be associated with possible single nucleotide polymorphisms (SNPs) in the *AOX1* gene, instability of the dimer, or deficiency of the essential molybdenum cofactor (Hartmann *et al.*, 2012, Hutzler *et al.*, 2012, Fu *et al.*, 2013, Hutzler *et al.*, 2014b), as well as extra-hepatic expression of AO (Kurosaki *et al.*, 1999, Moriwaki *et al.*, 2001, Nishimura and Naito, 2006, Terao *et al.*, 2016), although the contribution of these mechanisms are poorly understood. Consequently, promising drug candidates are routinely discarded or structurally modified to eliminate AO metabolism, often at the expense of pharmacological potency and/or selectivity.

While research has been conducted to evaluate human *in vitro* methods for direct scaling of AO-mediated clearance (Zientek *et al.*, 2010, Hutzler *et al.*, 2012, Hutzler *et al.*, 2014b), studies investigating allometric scaling approaches are limited. Allometric scaling of *in vivo* plasma clearance in nonclinical species is commonly used to predict human total body clearance of drugs eliminated renally and/or via hepatic metabolism (Mahmood, 2007). However, the aforementioned differences observed in AO expression and activity of species commonly employed in allometric scaling (particularly dog) have resulted in decreased confidence in the utility of this method to predict AO-mediated clearance. Interestingly, similar to AO, metabolism mediated by uridine diphosphate-glucuronosyltransferases (UGTs) has been found to vary with species, yet success in predicting human clearance of UGT-metabolized drugs with multispecies allometry (MA) and single-species scaling (SSS) has been demonstrated (Deguchi *et al.*, 2011). Furthermore, while rat underestimated the

human plasma clearance of the AO substrate BIBX1382, a report by Hutzler et al. demonstrated comparable BIBX1382 plasma clearance (as a percentage of liver blood flow) between cynomolgus monkey and human, indicating SSS with monkey may be useful in predicting the clearance of drugs subject to AO metabolism (Hutzler *et al.*, 2014a). Choughule et al., however, reported that relative hepatic intrinsic clearance (CL_{int}) mediated by AO in human, rhesus monkey, and guinea pig cytosol was substrate-dependent, suggesting that no single species could be reliably employed to consistently predict human clearance (Choughule *et al.*, 2013b). Given that the ability to successfully predict human clearance of AO substrates by allometry using a particular species (or combination of species) is likely to be substrate-dependent in nature, we sought to investigate the utility of scaling *in vitro* CL_{int} of AO substrates with allometry to human *in vitro* CL_{int} as a tool to determine which species (or combination of species) may be suitable for conducting traditional allometric scaling of *in vivo* clearance. Specifically, the *in vitro* CL_{int} of five compounds (Figure 1) known to be cleared either predominantly or partially by AO in human was determined in hepatic S9 from multiple nonclinical species known to express hepatic AO (mouse, rat, guinea pig, cynomolgus monkey, rhesus monkey, and minipig). Subsequently, CL_{int} obtained from multispecies hepatic S9 incubations was subjected to MA or SSS to predict human *in vitro* hepatic CL_{int}, and a folderror analysis was used to evaluate which species may be most suitable for estimating human *in vivo* clearance. In addition, we estimated $F_{m,AO}$ (fraction of metabolism mediated by AO) and hepatic extraction ratio (E) in each species (*in vitro*) to understand the potential influence of these variables on the accuracy of prediction by the scaling methods presented herein.

Materials and Methods

Materials

Potassium phosphate, formic acid, NADPH, $MgCl_2$, zaleplon, O^6-benzylguanine, and hydralazine hydrochloride were purchased from Sigma-Aldrich (St. Louis, MO). Zoniporide dihydrochloride, BIBX1382 dihydrochloride, and SGX523 were purchased from Tocris Bioscience (R&D Systems, Minneapolis, MN). Pooled human hepatic S9 (150-donor, mixed gender pool) was obtained from BD Biosciences (San Diego, CA), and male Sprague-Dawley rat (n=36 pool), cynomolgus monkey (n=2, pool), and CD-1 mouse (n=170 pool) hepatic S9 were obtained from Corning Inc. (Tewksbury, MA). Male rhesus monkey (n= 6 pool) and Hartley guinea pig (n=50 pool) hepatic S9 were purchased from XenoTech (Lenexa, KS), and male Gottingen minipig (n= 7 pool) hepatic S9 was purchased from BioreclamationIVT (Baltimore, MD). All solvents used for bioanalysis were purchased from Sigma-Aldrich or Fisher Scientific (Waltham, MA) and were of high-performance liquid chromatography (HPLC) grade.

Incubations with Multispecies Hepatic S9 Fractions

Substrates (1 μM) were incubated at 37°C for 60 minutes in a potassium phosphatebuffered reaction (100 mM, pH 7.4) containing hepatic S9 from human (mixed gender) or male mouse, rat, guinea pig, cynomolgus monkey, rhesus monkey, or minipig (2.5 mg/mL; +/− NADPH, 1 mM) and $MgCl_2$ (3 mM), with preincubation in the presence or absence of hydralazine (50 μM) for estimation of fraction metabolized by AO ($F_{m,AO}$). Reactions were

initiated with addition of substrate, and at designated times (t = 0, 7, 15, 30, 45, and 60 min), aliquots were removed and precipitated with ice-cold acetonitrile containing an internal standard (carbamazepine, 50 nM). The mixture was centrifuged at 3500 rcf for 5 min and resulting supernatants diluted with water in preparation for LC/MS/MS analysis of substrate depletion, by monitoring the analyte/internal standard peak area ratio.

Liquid Chromatography-Mass Spectrometry Analysis

The extent of substrate depletion in S9 fractions was determined employing LC/MS/MS analysis with an electrospray ionization enabled Sciex API-4000 triple quadrupole instrument (Sciex, Foster City, CA) that was coupled to LC-10AD pumps (Shimadzu, Columbia, MD) and a CTC PAL autosampler (Leap Technologies, Carrboro, NC). Analytes were separated by gradient elution using a Fortis C18 column (3 × 50 mm, 3 μm; Fortis Technologies Ltd., Cheshire, UK) warmed to 40°C. Mobile phase A was 0.1% formic acid in water (pH unadjusted); mobile phase B was 0.1% formic acid in acetonitrile, and the flow rate was 0.5 mL/min. Mass spectral analyses were performed using multiple reaction monitoring (MRM), with transitions and voltages specific for each analyte using a Turbo Ion Spray source (source temp 500°C) in positive ionization mode (5.0 kV spray voltage). MRM transitions were the following: zaleplon (*m/z* 306→236), O^6-benzylguanine (*m/z* 242→91), zoniporide (*m/z* 321→262), BIBX1382 (*m/z* 388→98), SGX523 (*m/z* 360→160), and carbamazepine (*m/z* 237 → 194). Data were analyzed using Sciex Analyst 1.5.1 software.

Data Analysis

Intrinsic Clearance (CL_{int})—*In vitro* hepatic intrinsic clearance (CL_{int}, mL/min/kg) for each species was extrapolated from hepatic S9 using the substrate depletion method and eq. 1 (Zientek *et al.*, 2010):

$$CL_{int} = \frac{ln2}{t_{1/2}\,(min)} \times \frac{mL}{2.5\ mg\ protein_{S9}} \times \frac{120.7\ mg\ protein_{S9}}{g\ liver\ weight} \times \frac{(A) g\ liver\ weight}{kg\ body\ weight} \quad (1)$$

The scaling factor, A, for each species is listed in Supplemental Table 1. CL_{int} was not calculated if the mean ln[C] versus time slope was not significantly different from zero (determined using GraphPad Prism version 5.04 by an F test with a significance level of $p < 0.05$) or if the slope was exclusively dependent on the terminal time point in order to be considered different from zero.

Hepatic Clearance (CL_{HEP})

Hepatic clearance (CL_{HEP}, mL/min/kg) was estimated using eq. 2, according to the wellstirred model, uncorrected for fraction unbound in plasma (Obach, 1999):

$$CL_{HEP} = \frac{Q_H \times CL_{int}}{Q_H + CL_{int}} \quad (2)$$

Where Q_H is species specific hepatic blood flow (Supplemental Table 1) and CL_{int} is the intrinsic clearance calculated from eq. 1. Protein binding was purposely not incorporated into CL_{HEP} estimations, as the intent of the CL_{HEP} estimations was not to scale *in vitro* CL_{int} to *in vivo* clearance, but rather to compare the relative extent of metabolism-mediated clearance across species (via estimation of the hepatic extraction ratio, eq. 3 below).

Hepatic Extraction Ratio (E)

The estimated hepatic extraction (E) was calculated using eq 3:

$$E = \frac{CL_{HEP}}{Q_H} \quad (3)$$

Estimation of fraction metabolized by AO ($F_{m,AO}$)

The $F_{m,AO}$ of the five compounds was estimated for each species. Hydralazine has been reported as a specific AO inhibitor suitable for use in determination of $F_{m,AO}$ (Strelevitz *et al.*, 2012). Utilizing this method in hepatic S9 fractions, incubations were fortified with NADPH in the presence or absence of hydralazine, and eq. 4 (method A) was applied to estimate the $F_{m,AO}$:

$$F_{m,AO(A)} = \frac{CL_{int} - CL_{int(+Hyd)}}{CL_{int}} \quad (4)$$

where CL_{int} is the intrinsic clearance in S9 fortified with NADPH and $CL_{int\ (+Hyd)}$ is the intrinsic clearance in S9 containing both NADPH and hydralazine. Alternatively, the $F_{m,AO}$ can also be estimated with eq. 5 (method B), utilizing S9 in the absence of NADPH (AO catalytic activity is NADPH-independent):

$$F_{m,AO\ (B)} = \frac{CL_{int\ (no\ NADPH)} - CL_{int\ (no\ NADPH+Hyd)}}{CL_{int}} \quad (5)$$

where $CL_{int\ (no\ NADPH)}$ is the intrinsic clearance in S9 without NADPH and $CL_{int\ (no\ NADPH+Hyd)}$ is the intrinsic clearance in S9 containing hydralazine without NADPH. In some cases, low turnover prevented an estimation of CL_{int} in S9 incubations containing NADPH and hydralazine ($CL_{int\ (+Hyd)} = 0$) or in S9 incubations absent NADPH ($CL_{int\ (no\ NADPH)} = 0$), which results in an $F_{m,AO}$ estimation equal to 1 by method A or 0 by method B, respectively. Due to this limitation, both methods A and B were used to approximate $F_{m,AO}$. In addition, agreement between the two methods provides more confidence in the estimate. In some cases low turnover prevented a calculation of $F_{m,AO}$ by both methods A and B.

Multi-species Allometry (MA) and Single-Species Scaling (SSS)

For allometric scaling of *in vitro* hepatic intrinsic clearance (CL_{int}), the *in vitro* values obtained from incubations of hepatic S9 from preclinical species were allometrically scaled to predict human hepatic S9 $CL_{int.}$ The simple allometric equation (eq. 6) was applied for predictions using 3 or 4 species:

$$CL_{int}\ (mL/min) = a \times W^{b} \quad (6)$$

where CL_{int} is the predicted intrinsic clearance, W is body weight, and a and b are the allometric coefficient and exponent, respectively. The coefficient and exponents a and b were obtained from a plot of CL_{int} versus body weight (W) (Supplemental Figure 1). A standard body weight for each species was used in the analyses (Supplemental Table 1). Following the same principle, eq. 7 was applied in single-species scaling (SSS) analyses, using a fixed exponent of 0.75, which has been proposed for use in SSS of PK parameters based on the understanding that many physiological factors including basal metabolic rate and passive renal clearance may be scaled using this exponent (Hosea *et al.*, 2009):

$$CL_{int\ (human)}\ (mL/min) = CL_{int\ (animal)} \times \frac{W_{human}^{0.75}}{W_{animal}} \quad (7)$$

Success Criteria

The success of each prediction method was assessed by calculation of the average absolute fold-error (AAFE) and the average fold-error (AFE), described by eq. 8 and 9, respectively (Obach *et al.*, 1997, Tang *et al.*, 2007),

$$AAFE = 10^{\frac{\sum|log(fold\ error)|}{N}} \quad (8)$$

$$AFE = 10^{\frac{\sum log(fold\ error)}{N}} \quad (9)$$

where N equals the total number of compounds, and fold-error (eq. 10) is the ratio of the predicted clearance (CL_{pred}) to the observed clearance (CL_{obs}),

$$fold\ error = \frac{CL_{pred}}{CL_{obs}} \quad (10)$$

where CL_{obs} represents the human CL_{int} (obtained using human hepatic S9, eq. 1) and CL_{pred} equals the predicted human hepatic S9 CL_{int} scaled from either MA or SSS of CL_{int}

obtained using hepatic S9 of preclinical species. AFE is equal to the geometric mean of the fold-error and represents a measurement of the overall bias in both directions (above or below the reference value of 1), whereas the AAFE gives both over-predictions and under-predictions equal value. Therefore, the overall bias of the prediction method towards under- or over-prediction is represented by the AFE, and the AAFE is an unbiased representation of the fold-error. An AAFE of ≤ 3 was considered successful; this criteria is in line with a convention reported in a recent PhRMA consensus paper by Ring et.al., identifying a < 2-, < 3- and <10-fold criteria in the identification of successful scaling methods (>10-fold criteria considered unsuccessful) (Ring *et al.*, 2011). The percentage of compounds within 2-fold-error (fold-error = 0.5–2.0) and 3-folderror (fold-error = 0.33–3.0) was also considered when assessing each method.

SSS Correlation with F_m or E

The fold-error for *in vitro* SSS CL_{int} predictions was plotted against the animal:human ratio of either $F_{m,AO}$ or E, with correlation coefficients (r^2) determined using GraphPad Prism version 5.04. $F_{m,AO}$ estimates calculated by method B were used for the analysis (except $F_{m,AO}$ of zaleplon in mouse and minipig because method B resulted in $F_{m,AO} = 0$ due to low turnover; estimates calculated from method A were instead used in these two instances). $F_{m,AO}$ of zaleplon in rat, O^6-benzylguanine in mouse, rat, and minipig, and BIBX1382 in mouse could not be determined by either method and were thus excluded from the analysis. $F_{m,AO}$ estimations > 1, were assumed to be equal to 1. No data were excluded from the analysis involving E.

For comparison to another non-cytochrome P450 pathway, similar correlation analyses were performed using *in vivo* data derived from a report by Deguchi et al. of SSS to predict human CL_p of uridine diphosphate-glucuronosltransferase (UGT) substrates (Deguchi *et al.*, 2011). For twelve UGT substrates, Deguchi et al. reported CL_p in each species (mouse, rat, monkey, and dog), human predictions of CL_p obtained from SSS, and $F_{m,UGT}$ in each species (estimated from *in vivo* production of glucuronide metabolites excreted into the bile and urine). For our correlation analyses using UGT substrate data from Deguchi et al., fold-errors of the SSS predictions were calculated as described above in eq. 10 from the observed human CL_p values and SSS CL_p predictions reported by Deguchi et al. $F_{m,UGT}$ was not reported by Deguchi et al for imipramine in mouse, nor was it reported for levofloxacin and telmisartan in human, resulting in exclusion of levofloxacin and telmisartan from the $F_{m,UGT}$ analysis. Similar to the correlation analysis involving E, an analysis was conducted using CL_p as a percentage of Q_H obtained from Deguchi et al's report. Eq. 3 was adapted to calculate CL_p as a percentage of Q_H using CL_p values reported by Deguchi et al. and species-specific hepatic blood flow, resulting in eq. 11:

$$CL_p \text{ as a percentage of } Q_H = \frac{CL_p}{Q_H} \quad (11)$$

When CL_p is exclusively mediated by hepatic elimination, this value (CL_p as a percentage of Q_H) will be equal to E. If extra-hepatic elimination is present, this value will be greater than

E. Therefore, levofloxacin and furosemide, which are predominantly excreted unchanged in the urine, were excluded from this analysis.

Results

Intrinsic clearance in hepatic S9 fractions and relationship to hepatic extraction ratio

Considering the test articles employed in the present investigation are metabolized by multiple drug metabolizing enzymes, namely P450 enzymes and aldehyde oxidase (AO), we limited the sub cellular fraction employed in the *in vitro* pharmacokinetic assays to S9 fractions (containing both cytosol/AO and microsomes/P450). Importantly, the ability to attenuate the contribution(s) of P450 enzymes by limiting co-factor fortification (i.e., NADPH) was of utmost importance in the determination of the total contribution of these individual enzymes in the clearance of the test articles *in vitro*, and towards the determination of a fraction-metabolized by AO ($F_{m,AO}$; *vide infra*). The intrinsic clearance (CL_{int}) estimates measured in hepatic S9 fractions of human and nonclinical species are summarized in Table 1. These data represent estimates from incubations in the presence of NADPH, thus encompassing clearance mediated by NADPH-independent (e.g. AO) as well as any NADPH-dependent (e.g. P450) pathways. CL_{int} was converted to hepatic clearance (CL_{HEP}) according to equation 2 for the purpose of estimating the hepatic extraction ratio (E), according to equation 3 (data summarized in Table 2). CL_{int} estimates for zaleplon were low for all species, with E estimated to be ≤ 0.32 in each species. O^6-benzylguanine CL_{int} estimates were moderate in human, monkey, and guinea pig and lower in rat, mouse and minipig, resulting in E estimates that ranged from approximately 0.1 (rat, mouse, minipig) to approximately 0.5 (human, cynomolgus, and guinea pig). Conversely, zoniporide was moderately cleared in human, monkey, guinea pig, and minipig S9 incubations (E = 0.41 – 0.59), while it was rapidly cleared in incubations with rat and mouse S9 (E = 0.87 and 0.79, respectively). Estimated CL_{int} of BIBX1382 was high in human, monkey, and minipig (E = 0.72 – 0.83), moderate in guinea pig (E = 0.54), and low in rat and mouse (E = 0.30 and 0.27, respectively). SGX523 exhibited low-moderate clearance in all species, with E ranging from 0.25 – 0.50. Consistent with the observations of others (Choughule *et al.*, 2013a), no single species was fully representative of human when considering E for each compound, but rather substratedependence was observed. However, E estimated in cynomolgus and rhesus monkey was most similar to human overall, followed by guinea pig and minipig; rat and mouse generally provided a poorer representation of human E. These data highlight the need to conduct an interspecies evaluation for selection of appropriate species for human PK prediction

Estimation of $F_{m,AO}$ in hepatic S9 fractions

Table 3 summarizes $F_{m,AO}$ estimated for each compound in each species using methods A and B (eq. 4 and 5, respectively). $F_{m,AO}$ obtained for O^6-benzylguanine, zaleplon, zoniporide, and BIBX1382 in human is consistent with previous reports (Hutzler *et al.*, 2012, Strelevitz *et al.*, 2012). In addition, with a few exceptions, the two methods used to estimate human $F_{m,AO}$ generally produced similar values, providing more confidence in these estimates. It is important to note that the lower the rate of depletion, the less accurate the estimation of CL_{int}, (and thus, $F_{m,AO}$) using the substrate depletion method due to

difficulty in distinguishing legitimate metabolism-mediated depletion from biological or bioanalytical variability in detection (Di and Obach, 2015, Hutzler *et al.*, 2015). For example, in isolated incidences, low turnover resulted in an $F_{m,AO}$ estimation of 1 or 0, by method A or B, respectively (e.g. estimation of zaleplon $F_{m,AO}$ in rat), in which case, $F_{m,AO}$ was not reported. Ideally, under circumstances of low turnover, CL_{int} could be estimated via metabolite formation and determination of Michaelis-Menten parameters ($CL_{int} = V_{max} / K_m$); however, this method requires authentic standards of each major metabolite (e.g. AO and P450-mediated metabolites) contributing to the overall clearance.

Zaleplon $F_{m,AO}$.

CL_{int} of zaleplon in human S9 incubations with hydralazine could not be measured; however, a value of 0.71 was determined using method B, consistent with previous reports (Strelevitz *et al.*, 2012). Cynomolgus monkey, rhesus monkey, and guinea pig demonstrated similar $F_{m,AO}$ to human, with estimates ranging between 0.42–0.70, while mouse and minipig estimates were ≤ 0.22. Turnover of zaleplon in rat S9 was only measurable in incubations with NADPH absent hydralazine, preventing an $F_{m,AO}$ estimate from being obtained.

O^6-benzylguanine $F_{m,AO}$.

A high $F_{m,AO}$ (≥ 0.70) was estimated for O^6-benzylguanine in all species except rat, mouse, and minipig, which could not be determined due to low turnover of the compound. As was the case for zaleplon in rat S9 incubations, a lack of measurable turnover of O^6benzylguanine in rat, mouse, and minipig S9 incubations in the presence of both NADPH and hydralazine as well as incubations absent NADPH prevented estimation of $F_{m,AO}$.

Zoniporide $F_{m,AO}$.

A high $F_{m,AO}$ (> 0.70) for zoniporide was estimated in all species. In human, rat, and guinea pig, NADPH-independent clearance of zoniporide was not completely inhibited by hydralazine. Literature reports indicate hydrolysis as a secondary metabolism pathway of zoniporide (Dalvie *et al.*, 2010, Strelevitz *et al.*, 2012), which may account for this observation.

BIBX1382 $F_{m,AO}$.

$F_{m,AO}$ for BIBX1382 was estimated to be ≥ 0.70 by both methods in all species except rat and mouse. BIBX1382 reportedly undergoes some degree of P450 2D6-mediated metabolism (Dittrich *et al.*, 2002), and it has been reported that hydralazine may exert mild human 2D6 inhibition (Strelevitz *et al.*, 2012, Zientek and Youdim, 2015), in which case method A could potentially estimate an inflated $F_{m,AO}$; however, both methods A and B resulted in the same $F_{m,AO}$ estimation in human, suggesting that either P450 2D6-mediated clearance was insignificant, or hydralazine did not inhibit this pathway. This result is in agreement with a previous report phenotyping BIBX1382 clearance in human hepatocytes, where substrate depletion was predominantly mediated by AO (Hutzler *et al.*, 2012). Interestingly, CL_{int} in rat S9 incubations fortified with NADPH was only slightly inhibited by hydralazine (decreased from 29 to 25 mL/min/kg), suggestive of predominantly NADPH-

dependent clearance; however, in incubations absent NADPH, a CL_{int} of 19 mL/min/kg still remained. This finding indicates the possibility that the cytosolic enzyme xanthine oxidase (XO) may mediate part of the NADPH-independent clearance in rat S9 since XO is not inhibited by hydralazine; however, no measurable substrate depletion was observed in incubations containing hydralazine without NADPH. Minor depletion of BIBX1382 CL_{int} was observed in human S9 incubations containing hydralazine without NADPH, but no other species exhibited measurable depletion under these conditions.

SGX523 $F_{m,AO}$.

Considerable variability between the two methods was observed in the $F_{m,AO}$ of SGX523 in some species (e.g. guinea pig), but overall a low-moderate $F_{m,AO}$ was estimated in all species (range of 0.03 – 0.68). In some species (mouse, rhesus, and guinea pig), not all NADPHindependent activity was inhibited by hydralazine, indicating potential involvement of XO; Diamond et al. reported an absence of XO metabolism in formation of the SGX523 oxidative metabolite M11 in human and cynomolgus S9, but rather that the metabolite was solely attributed to AO (Diamond *et al.*, 2010). It is possible that the challenges associated with low substrate turnover, as described previously, contributed to our observations.

In general, the $F_{m,AO}$ calculated by the two different methods were in better agreement for compounds/species exhibiting more rapid clearance, and thus, more confidence can be placed in the accuracy of these estimations. Monkey and guinea pig demonstrated $F_{m,AO}$ values most similar to human. However, because low turnover prevented an $F_{m,AO}$ calculation for some compounds in mouse, rat, and minipig, it is unclear how closely these species replicate human $F_{m,AO}$.

Prediction of human hepatic S9 clearance by multi-or single species allometry

Intrinsic clearance estimates from hepatic S9 incubations from mouse, rat, guinea pig, cynomolgus, rhesus, and minipig were employed in various combinations of 3 or 4 species for allometric scaling (MA) as well as individually for direct extrapolation from a single-species (SSS). Human CL_{int} values predicted from MA and SSS were compared to CL_{int} measured in incubations with human hepatic S9. The overall performance of each method is summarized in Supplemental Table 2 (MA) and Table 4 (SSS), and plots of the observed CL_{int} for each compound versus the human CL_{int} predicted by each method are displayed in Supplemental Figure 2 (MA) and Figure 2 (SSS) (see also tabulated data in Supplemental Tables 3 and 4, along with the allometric exponents obtained for each MA method).

MA of CL_{int}.

An AAFE of ≤ 2.0 was obtained from all of the 4-species combinations and from the rhesus/rat/mouse combination, with rhesus/rat/mouse yielding the lowest AAFE (1.7) and 80% of the five compounds predicted within 2-fold of the experimentally measured human S9 CL_{int} (Supplemental Table 2). Only two combinations, cynomolgus/rat/mouse and cynomolgus/guinea pig/mouse, resulted in AAFE of > 3.0 (3.3-fold and 3.5-fold respectively). SGX523 is the only compound of the five for which a fold-error of < 3 could not be obtained by at least one of the species combinations; however, the minipig/rhesus/guinea pig combination yielded a fold-error of 3.0 (Supplemental Figure 2, Supplemental

Table 3). Interestingly, all but one of the species combinations (minipig/rat/mouse) had an AFE of ≥ 1.0, indicating that the predictions were biased towards over-prediction rather than under-prediction. This clearly was not the case in every instance, however, particularly for O^6-benzylguanine and zoniporide (Supplemental Figure 2, Supplemental Table 3).

SSS of CL_{int}.

Single-species scaling (SSS) has previously been reported to be as accurate or better than MA in predicting human pharmacokinetics, regardless of clearance mechanism, including P450 and non-P450 metabolism (Hosea *et al.*, 2009). Therefore, we chose to investigate this method in addition to MA for prediction of human S9 CL_{int}. SSS predictions yielded AAFEs of ≤ 2.0 when scaling from cynomolgus and rhesus monkey, guinea pig, and minipig S9 CL_{int}, with 80% of compounds predicted within 3-fold-error for cynomolgus, guinea pig, and minipig, and 100% for rhesus (Table 4; Figure 2). The compound falling outside of 3-fold-error differed for each species—SGX523 for cynomolgus, BIBX1382 for guinea pig, and O^6-benzylguanine for minipig (Figure 2, Supplemental Table 4). AAFEs for rat and mouse were 4.1 and 3.8, respectively, with only 40% and 60% of compounds predicted within 3-fold-error, respectively. A tendency towards under-prediction via SSS was exhibited in all species except monkey, which had AFEs of 1.6 (cynomolgus) and 1.2 (rhesus).

Relationship of F_m or E to SSS prediction accuracy

Based on their studies examining allometric scaling of UGT substrates, Deguchi et al. reported that overall $F_{m,UGT}$ values in monkey were more similar to human than other species evaluated, concluding that this likely contributed to a higher rate of prediction accuracy from monkey SSS relative to the other species investigated (mouse, rat, and dog) (Deguchi *et al.*, 2011). Likewise, we observed similar $F_{m,AO}$ values between monkey and human, as well as better overall success with predictions from monkey SSS. However, a similar $F_{m,AO}$ between animals and human did not always translate to a more accurate CL_{int} prediction. Furthermore, in Deguchi's report it can also be observed when comparing individual $F_{m,UGT}$ of each compound for each species with predicted CL_p by SSS, that a species exhibiting a similar $F_{m,UGT}$ to human did not always yield a more accurate prediction versus another species displaying a $F_{m,UGT}$ substantially different from human (Deguchi *et al.*, 2011). In some cases however we observed a similar E between human and a given species despite a divergence in $F_{m,AO}$, suggesting that other metabolism pathways are contributing to compensate for the lacking AO pathway, resulting in a reasonable human CL_{int} prediction. To evaluate the relationship between $F_{m,AO}$ or E and the accuracy of prediction by SSS, the CL_{int} prediction fold-error by SSS was plotted against the animal:human ratio of either $F_{m,AO}$ or E (Figure 3A and C) A correlation was not observed between the animal:human ratio of $F_{m,AO}$ and the fold-error in the CL_{int} predicted from SSS ($r^2 = 0.0051$). However, a positive correlation was observed between SSS CL_{int} prediction fold-error and E ($r^2 = 0.6488$). To determine if similar trends existed among the 12 UGT substrates evaluated by Deguchi et al., data were obtained from this report (Deguchi *et al.*, 2011) to plot the CL_p prediction fold-error by SSS against the animal:human ratio of $F_{m,UGT}$ (Figure 3B) or against the animal:human ratio of CL_p as a percentage of Q_H (Figure 3D). Because CL_p as a percentage of Q_H will be equal to E when clearance is mediated by hepatic elimination, we excluded UGT substrates that are predominantly cleared renally.

Once again, correlation with $F_{m,UGT}$ was poor ($r^2 = 0.00034$), but was strong with CL_p as a percentage of Q_H ($r^2 = 0.9573$). Overall, these data suggest that the fold-error in clearance prediction by SSS is more closely associated with the overall hepatic extraction efficiency than the F_m between human and a given species.

SSS of zoniporide and BIBX1382 CL_p

In vivo plasma clearance (CL_p) reported in the literature for zoniporide and BIBX1382 in mouse, rat, and cynomolgus monkey (Dalvie *et al.*, 2013, Hutzler *et al.*, 2014a) were subjected to SSS to predict human CL_p. These data are displayed in Table 5, alongside *in vitro* data for comparison. When comparing zoniporide *in vitro* data (E, $F_{m,AO}$, and SSS human CL_{int} prediction) of mouse, rat, cynomolgus monkey, and human, the species exhibiting the most similarity to human across all data is cynomolgus monkey. Accordingly, SSS of CL_p using cynomolgus monkey resulted in a more accurate human zoniporide CL_p prediction (15.2 mL/min/kg) versus mouse and rat (39.2 and 62.7, respectively) relative to the observed human CL_p (21 mL/min/kg). Comparison of *in vitro* data for BIBX1382 also demonstrated greater similarities between human and cynomolgus monkey relative to mouse and rat. Likewise, SSS of CL_p using cynomolgus monkey yielded a better human BIBX1382 CL_p prediction (56 mL/min/kg) versus mouse and rat (7.2 and 13.4, respectively) relative to the observed human CL_p (25–55 mL/min/kg).

Discussion

The general assumption in the utility of traditional allometric scaling to predict human clearance is that it requires conserved drug elimination mechanisms across species. Accordingly, where AO-mediated clearance exists, confidence in this approach is lacking due to differences in AO expression and activity between human and preclinical species traditionally employed (e.g. mouse, rat, dog), resulting in limited studies examining allometry to predict human clearance of AO substrates. In the present investigation, human *in vitro* hepatic CL_{int} of five AO substrates was successfully predicted by MA and SSS with certain species, indicating the possibility that allometry may be useful for predicting human *in vivo* clearance of AO substrates when the appropriate species are utilized. Others have proposed that species expressing only the AOX1 isoenzyme in the liver (e.g. guinea pig, monkey) may serve as better species to estimate human AO-mediated metabolism versus species expressing both the AOX1 and AOX3 isoenzymes (e.g. rat, mouse) (Garattini and Terao, 2012). Consistent with this proposal, our *in vitro* data indicate that the hepatic CL_{int} of AO substrates may be scaled from preclinical species to human by SSS with monkey, guinea pig, and minipig with reasonable accuracy and precision, while this relationship does not appear to be consistent (highly substrate-dependent) when directly scaling from rat or mouse. However, even SSS with guinea pig, monkey, and minipig exhibited some degree of substrate-dependency, which was similarly reported by Choughule et al. with regard to guinea pig and rhesus monkey cytosolic CL_{int} of AO substrates DACA and phthalazine (Choughule *et al.*, 2013b). Given these observations, we propose that allometric scaling of *in vitro* hepatic CL_{int} may be beneficial for guiding selection of suitable species to be utilized for prediction of human *in vivo* clearance via allometry. In addition, we propose that species selection may be further aided by interspecies comparison of $F_{m,AO}$ and E estimated from *in*

vitro CL_{int}. Table 5 illustrates an example of this approach, where comparison of *in vitro* data (E, $F_{m,AO}$, and human CL_{int} prediction by SSS) indicates that SSS with cynomolgus monkey would be more appropriate than SSS with mouse or rat to estimate human CL_p of zoniporide and BIBX1382. Accordingly, when CL_p obtained from the literature was scaled to human CL_p via SSS with cynomolgus monkey, rat, or mouse (Table 5), SSS with cynomolgus monkey did in fact yield the most accurate estimate of human CL_p for both zoniporide and BIBX1382. These examples together support the proposed *in vitro* allometry approach as a potentially useful method to identify suitable nonclinical species for estimating human *in vivo* clearance via traditional allometry. Figure 4 depicts a flow chart summarizing this approach, which may prevent unnecessary PK studies in species that are not likely to reflect human PK. Furthermore, though beyond the scope of the present investigation, this approach may also benefit (in combination with *in vitro* biotransformation experiments) selection of appropriate species for toxicity testing.

A potential limitation to the utility of this *in vitro* allometry approach is the use of hepatic S9, which only represents clearance mediated by hepatic metabolism. Though the contribution of extrahepatic metabolism to total body clearance of AO-metabolized compounds is currently poorly understood, extrahepatic expression of AO has been demonstrated in human as well as nonclinical species (Kurosaki *et al.*, 1999, Moriwaki *et al.*, 2001, Nishimura and Naito, 2006, Terao *et al.*, 2016). Furthermore, differences in the *AOX1* mRNA levels observed in various tissues between humans and mice (Terao *et al.*, 2016) indicate tissue-specific expression patterns may not parallel across species. For example, Hutzler et al. demonstrated metabolism of BIBX1382 in lung and kidney S9 fractions of human and cynomolgus monkey (Hutzler *et al.*, 2014a), although species differences in the relative rates of elimination of BIBX1382 from these two tissues were noted. Indeed, human CL_p for four of the five substrates we evaluated are reported in the literature and were each under-represented by our CL_{HEP} estimates from human S9 incubations, including BIBX1382 (Table 6). This is not an uncommon observation, which may be attributed to extrahepatic metabolism, among other possibilities, such as SNPs or other sources of donor variability, *ex vivo* protein instability, or procedural differences in tissue procurement that may yield lot-to-lot variability in AO activity from commercial sources of S9 (Hartmann *et al.*, 2012, Hutzler *et al.*, 2012, Fu *et al.*, 2013, Hutzler *et al.*, 2014b). While our *in vitro* studies do not account for potential extrahepatic clearance which may occur *in vivo*, they were conducted under the assumption that hepatic AO-mediated metabolism is largely responsible for drug clearance, such that hepatic CL_{int} measurements will permit suitable species selection, even though the *in vitro* CL_{int} may underrepresent the total body clearance occurring *in vivo*. Accordingly, despite differences observed in elimination from extrahepatic S9 fractions of cynomolgus and human (Hutzler *et al.*, 2014a), SSS of cynomolgus CL_p of BIBX1382 still predicted the rapid CL_p observed in clinical pharmacokinetic studies (Table 5), and our *in vitro* assessments with hepatic S9 successfully identified cynomolgus as an appropriate species. Future research to establish species-specific tissue expression patters, mechanisms regulating AO expression, and importantly, to develop standardized *in vitro* scaling factors that can be used to estimate total organ clearance from *in vitro* CL_{int} in extra-hepatic tissues will all be critical steps towards understanding the potential contribution of extra-hepatic metabolism.

In addition to our *in vitro* allometry assessments, we evaluated the relationship between interspecies $F_{m,AO}$ or E and the fold-error of human CL_{int} prediction by SSS. Interestingly, comparison of prediction fold-errors by SSS with the animal:human ratio of either $F_{m,AO}$ or E revealed little correlation with $F_{m,AO}$, but a positive correlation with E; similar trends were also observed for UGT substrates when plotting SSS prediction fold-error of CL_p versus the animal:human ratio of $F_{m,UGT}$ or CL_p as a percentage of Q_H. We observed some examples where a discrepancy in $F_{m,AO}$ between human and animal did not preclude a similar E, which suggests a non-AO metabolism pathway may compensate for the lacking AO pathway to result in an overall similar hepatic extraction efficiency. For example, the $F_{m,AO}$ obtained for zaleplon was substantially higher in human (≥ 0.71) versus minipig (≤ 0.17), while the E between the two species was similar (human = 0.22, minipig = 0.16). Consequently, these data may indicate that compounds containing a mixed AO/P450 metabolism phenotype, or possessing P450 favorable sites in addition to the AO metabolism site, could help to enable allometric scaling approaches if alternate metabolism pathway(s) in certain species compensate for reduced AO-mediated clearance. Nonetheless, these observations suggest that there is not a strong relationship between F_m and the prediction fold-error by SSS or that methods to obtain F_m are not sufficiently accurate to observe this relationship. With regard to the present study, it should be noted that our $F_{m,AO}$ calculations assume that 50 μM hydralazine is adequate to selectively and completely inhibit AO metabolism, whereas the potency and selectivity of hydralazine is not known for all species studied. In addition, our $F_{m,AO}$ calculations are dependent on the ability to measure substrate depletion when turnover may be low, which presents an additional challenge in obtaining an accurate $F_{m,AO}$ estimate. Importantly, the challenge of low substrate turnover is not unique to the present AO investigation, as the P450 literature is replete with similar data generated for the purposes of scaling a particular PK parameter (such as clearance), and subsequently resulting in a successful model or simulation. Current research efforts among the drug metabolism community are focused on the development of novel *in vitro* models towards the resolution of this issue (Di and Obach, 2015, Hutzler *et al.*, 2015). Finally, four of the five compounds exhibited an $F_{m,AO}$ in human of ≥ 0.70. A larger data set consisting of compounds exhibiting a broader range of $F_{m,AO}$ would help to better understand the importance of this value to obtaining an accurate human hepatic clearance prediction by SSS.

For our *in vitro* allometry assessment, we included data obtained from minipig, which is gaining popularity in preclinical development (particularly safety testing) due to similarities in anatomy and physiology to humans, as well as advantages related to regulatory acceptability and animal welfare (Bode *et al.*, 2010, Ellegaard *et al.*, 2010, van der Laan *et al.*, 2010). With regard to drug metabolism, minipigs hold an advantage over dogs (concerning nonrodent/large animals) when AO is involved, as dogs are essentially devoid of AO activity in the liver (Dalgaard, 2015, Terao *et al.*, 2016). In addition, a recent report found minipig to be useful in allometric scaling of drugs mostly cleared by P450 or glucuronidation (Yoshimatsu *et al.*, 2016). For the present investigation, we chose to replace dog, which is commonly used for allometric scaling, with minipig, a species of similar body weight. Indeed, the use of minipig for MA enabled human S9 CL_{int} to be predicted with an AAFE of < 3, and SSS with minipig predicted CL_{int} within 3-fold for four out of five

substrates. However, as noted previously, the $F_{m,AO}$ of zaleplon was higher in human versus minipig, indicating that a non-AO metabolism pathway enabled the accurate human CL_{int} prediction (unlike monkey and guinea pig which demonstrated similar $F_{m,AO}$ to human). Along with substantial underprediction of O^6-benzylguanine human CL_{int} by minipig SSS, this observation highlights the potential substrate-dependency associated with this species. Interestingly, based on the AAFE and individual evaluation of fold-error for each of the five compounds, MA methods utilizing four species (including minipig) may prove to be more reliable than 3-species combinations, even though rat and mouse (which yielded poorer predictions by SSS) were included in the 4-species combinations (Supplemental Tables 2 and 3; Supplemental Figure 2). Evaluation of these species combinations *in vivo* will be important to fully understand this approach.

Conclusions

In summary, our data support prior postulations that guinea pig and monkey represent better models of AO-mediated drug clearance in human versus commonly employed nonclinical models such as rat or mouse (Garattini and Terao, 2012, Hutzler *et al.*, 2013, Hutzler *et al.*, 2014a), while reiterating that no single species should be expected to reflect human clearance of all AO substrates (Choughule *et al.*, 2013b, Hutzler *et al.*, 2013). Moreover, the minipig represents a large animal species to consider when investigating AO metabolism, particularly when employed in multispecies allometry and drug safety assessments of NCEs (Bode *et al.*, 2010, Ellegaard *et al.*, 2010, van der Laan *et al.*, 2010) Collectively, our data support the need for a multiple species assessment when gauging the intrinsic lability of new chemical entities (NCEs) towards AO metabolism and the projection of drug clearance in human, and we have offered a potentially useful *in vitro* approach to aid in selecting nonclinical species that may provide the best estimates of human clearance when evaluated *in vivo* (potentially reducing the number of unnecessary *in vivo* PK studies conducted in inappropriate species). While mechanisms behind variable AO activity and contributions of extra-hepatic metabolism remain important unanswered questions towards the implementation of standardized methods pertaining to AO-mediated drug disposition, application of the methodology presented herein would likely reduce the risk of encountering unexpected rapid AO-mediated clearance in clinical trials due to the use of inappropriate species for preclinical assessments.

Supplementary Material

Refer to Web version on PubMed Central for supplementary material.

Acknowledgements

This work was supported by the Pharmaceutical Research and Manufacturers of America Foundation (PhRMA Foundation Pre-Doctoral Fellowship); the National Institutes of Health under Grant T32GM07628.

References

Akabane T, Tanaka K, Irie M, Terashita S & Teramura T, 2011 Case report of extensive metabolism by aldehyde oxidase in humans: Pharmacokinetics and metabolite profile of FK3453 in rats, dogs, and humans. Xenobiotica, 41, 372–384. [PubMed: 21385103]

Bode G, Clausing P, Gervais F, Loegsted J, Luft J, Nogues V & Sims J, 2010 The utility of the minipig as an animal model in regulatory toxicology. J Pharmacol Toxicol Methods, 62, 196–220. [PubMed: 20685310]

Choughule KV, Barr JT & Jones JP, 2013a Evaluation of Rhesus Monkey and Guinea Pig Hepatic Cytosol Fractions as Models for Human Aldehyde Oxidase. Drug Metabolism and Disposition, 41, 1852–1858. [PubMed: 23918666]

Choughule KV, Barr JT & Jones JP, 2013b Evaluation of rhesus monkey and guinea pig hepatic cytosol fractions as models for human aldehyde oxidase. Drug Metab Dispos, 41, 1852–8. [PubMed: 23918666]

Dalgaard L, 2015 Comparison of minipig, dog, monkey and human drug metabolism and disposition. J Pharmacol Toxicol Methods, 74, 80–92. [PubMed: 25545337]

Dalvie D, Xiang C, Kang P & Zhou S, 2013 Interspecies variation in the metabolism of zoniporide by aldehyde oxidase. Xenobiotica, 43, 399–408. [PubMed: 23046389]

Dalvie D, Zhang C, Chen W, Smolarek T, Obach RS & Loi CM, 2010 Cross-species comparison of the metabolism and excretion of zoniporide: contribution of aldehyde oxidase to interspecies differences. Drug Metab Dispos, 38, 641–54. [PubMed: 20040581]

Deguchi T, Watanabe N, Kurihara A, Igeta K, Ikenaga H, Fusegawa K, Suzuki N, Murata S, Hirouchi M, Furuta Y, Iwasaki M, Okazaki O & Izumi T, 2011 Human Pharmacokinetic Prediction of UDP-Glucuronosyltransferase Substrates with an Animal Scale-Up Approach. Drug Metabolism and Disposition, 39, 820–829. [PubMed: 21282406]

Di L & Obach RS, 2015 Addressing the challenges of low clearance in drug research. AAPS J, 17, 352–7. [PubMed: 25567366]

Diamond S, Boer J, Maduskuie TP, Falahatpisheh N, Li Y & Yeleswaram S, 2010 Species-Specific Metabolism of SGX523 by Aldehyde Oxidase and the Toxicological Implications. Drug Metabolism and Disposition, 38, 1277–1285. [PubMed: 20421447]

Dittrich C, Greim G, Borner M, Weigang-Köhler K, Huisman H, Amelsberg A, Ehret A, Wanders J, Hanauske A & Fumoleau P, 2002 Phase I and pharmacokinetic study of BIBX 1382 BS, an epidermal growth factor receptor (EGFR) inhibitor, given in a continuous daily oral administration. European Journal of Cancer, 38, 1072–1080. [PubMed: 12008195]

Ellegaard L, Cunningham A, Edwards S, Grand N, Nevalainen T, Prescott M & Schuurman T, 2010 Welfare of the minipig with special reference to use in regulatory toxicology studies. J Pharmacol Toxicol Methods, 62, 167–83. [PubMed: 20621655]

Fu C, Di L, Han X, Soderstrom C, Snyder M, Troutman MD, Obach RS & Zhang H, 2013 Aldehyde oxidase 1 (AOX1) in human liver cytosols: quantitative characterization of AOX1 expression level and activity relationship. Drug Metab Dispos, 41, 1797–804. [PubMed: 23857892]

Garattini E & Terao M, 2012 The role of aldehyde oxidase in drug metabolism. Expert Opinion on Drug Metabolism & Toxicology, 8, 487–503. [PubMed: 22335465]

Hartmann T, Terao M, Garattini E, Teutloff C, Alfaro JF, Jones JP & Leimkuhler S, 2012 The impact of single nucleotide polymorphisms on human aldehyde oxidase. Drug Metab Dispos, 40, 856–64. [PubMed: 22279051]

Hosea NA, Collard WT, Cole S, Maurer TS, Fang RX, Jones H, Kakar SM, Nakai Y, Smith BJ, Webster R & Beaumont K, 2009 Prediction of Human Pharmacokinetics From Preclinical Information: Comparative Accuracy of Quantitative Prediction Approaches. The Journal of Clinical Pharmacology, 49, 513–533. [PubMed: 19299532]

Hutzler JM, Cerny MA, Yang YS, Asher C, Wong D, Frederick K & Gilpin K, 2014a Cynomolgus monkey as a surrogate for human aldehyde oxidase metabolism of the EGFR inhibitor BIBX1382. Drug Metab Dispos, 42, 1751–60. [PubMed: 25035284]

Hutzler JM, Obach RS, Dalvie D & Zientek MA, 2013 Strategies for a comprehensive understanding of metabolism by aldehyde oxidase. Expert Opinion on Drug Metabolism & Toxicology, 9, 153–168. [PubMed: 23231678]

Hutzler JM, Ring BJ & Anderson SR, 2015 Low-Turnover Drug Molecules: A Current Challenge for Drug Metabolism Scientists. Drug Metab Dispos, 43, 1917–28. [PubMed: 26363026]

Hutzler JM, Yang Y-S, Albaugh D, Fullenwider CL, Schmenk J & Fisher MB, 2012 Characterization of Aldehyde Oxidase Enzyme Activity in Cryopreserved Human Hepatocytes. Drug Metabolism and Disposition, 40, 267–275. [PubMed: 22031625]

Hutzler JM, Yang Y-S, Brown C, Heyward S & Moeller T, 2014b Aldehyde Oxidase Activity in Donor-Matched Fresh and Cryopreserved Human Hepatocytes and Assessment of Variability in 75 Donors. Drug Metabolism and Disposition, 42, 10901097.

Kurosaki M, Demontis S, Barzago MM, Garattini E & Terao M, 1999 Molecular cloning of the cDNA coding for mouse aldehyde oxidase: tissue distribution and regulation in vivo by testosterone. Biochem J, 341 (Pt 1), 71–80. [PubMed: 10377246]

Mahmood I, 2007 Application of allometric principles for the prediction of pharmacokinetics in human and veterinary drug development. Adv Drug Deliv Rev, 59, 1177–92. [PubMed: 17826864]

Moriwaki Y, Yamamoto T, Takahashi S, Tsutsumi Z & Hada T, 2001 Widespread cellular distribution of aldehyde oxidase in human tissues found by immunohistochemistry staining. Histol Histopathol, 16, 745–53. [PubMed: 11510964]

Nishimura M & Naito S, 2006 Tissue-specific mRNA expression profiles of human phase I metabolizing enzymes except for cytochrome P450 and phase II metabolizing enzymes. Drug Metab Pharmacokinet, 21, 357–74. [PubMed: 17072089]

Obach RS, 1999 Prediction of human clearance of twenty-nine drugs from hepatic microsomal intrinsic clearance data: An examination of in vitro half-life approach and nonspecific binding to microsomes. Drug Metab Dispos, 27, 1350–9. [PubMed: 10534321]

Obach RS, Baxter JG, Liston TE, Silber BM, Jones BC, Macintyre F, Rance DJ & Wastall P, 1997 The Prediction of Human Pharmacokinetic Parameters from Preclinical and In Vitro Metabolism Data. Journal of Pharmacology and Experimental Therapeutics, 283, 46–58. [PubMed: 9336307]

Pryde DC, Dalvie D, Hu Q, Jones P, Obach RS & Tran T-D, 2010 Aldehyde Oxidase: An Enzyme of Emerging Importance in Drug Discovery. Journal of Medicinal Chemistry, 53, 8441–8460. [PubMed: 20853847]

Ring BJ, Chien JY, Adkison KK, Jones HM, Rowland M, Jones RD, Yates JW, Ku MS, Gibson CR, He H, Vuppugalla R, Marathe P, Fischer V, Dutta S, Sinha VK, Bjornsson T, Lave T & Poulin P, 2011 PhRMA CPCDC initiative on predictive models of human pharmacokinetics, part 3: comparative assessement of prediction methods of human clearance. J Pharm Sci, 100, 4090–110. [PubMed: 21541938]

Strelevitz TJ, Orozco CC & Obach RS, 2012 Hydralazine As a Selective Probe Inactivator of Aldehyde Oxidase in Human Hepatocytes: Estimation of the Contribution of Aldehyde Oxidase to Metabolic Clearance. Drug Metabolism and Disposition, 40, 1441–1448. [PubMed: 22522748]

Tang H, Hussain A, Leal M, Mayersohn M & Fluhler E, 2007 Interspecies prediction of human drug clearance based on scaling data from one or two animal species. Drug Metab Dispos, 35, 1886–93. [PubMed: 17646280]

Terao M, Romao MJ, Leimkuhler S, Bolis M, Fratelli M, Coelho C, Santos-Silva T & Garattini E, 2016 Structure and function of mammalian aldehyde oxidases. Arch Toxicol, 90, 753–80. [PubMed: 26920149]

Van Der Laan JW, Brightwell J, Mcanulty P, Ratky J & Stark C, 2010 Regulatory acceptability of the minipig in the development of pharmaceuticals, chemicals and other products. J Pharmacol Toxicol Methods, 62, 184–95. [PubMed: 20601024]

Yoshimatsu H, Konno Y, Ishii K, Satsukawa M & Yamashita S, 2016 Usefulness of minipigs for predicting human pharmacokinetics: Prediction of distribution volume and plasma clearance. Drug Metab Pharmacokinet, 31, 73–81. [PubMed: 26776246]

Zhang X, Liu HH, Weller P, Zheng M, Tao W, Wang J, Liao G, Monshouwer M & Peltz G, 2011 In silico and in vitro pharmacogenetics: aldehyde oxidase rapidly metabolizes a p38 kinase inhibitor. Pharmacogenomics J, 11, 15–24. [PubMed: 20177421]

Zientek M, Jiang Y, Youdim K & Obach RS, 2010 In Vitro-In Vivo Correlation for Intrinsic Clearance for Drugs Metabolized by Human Aldehyde Oxidase. Drug Metabolism and Disposition, 38, 1322–1327. [PubMed: 20444863]

Zientek MA & Youdim K, 2015 Reaction phenotyping: advances in the experimental strategies used to characterize the contribution of drug-metabolizing enzymes. Drug Metab Dispos, 43, 163–81. [PubMed: 25297949]

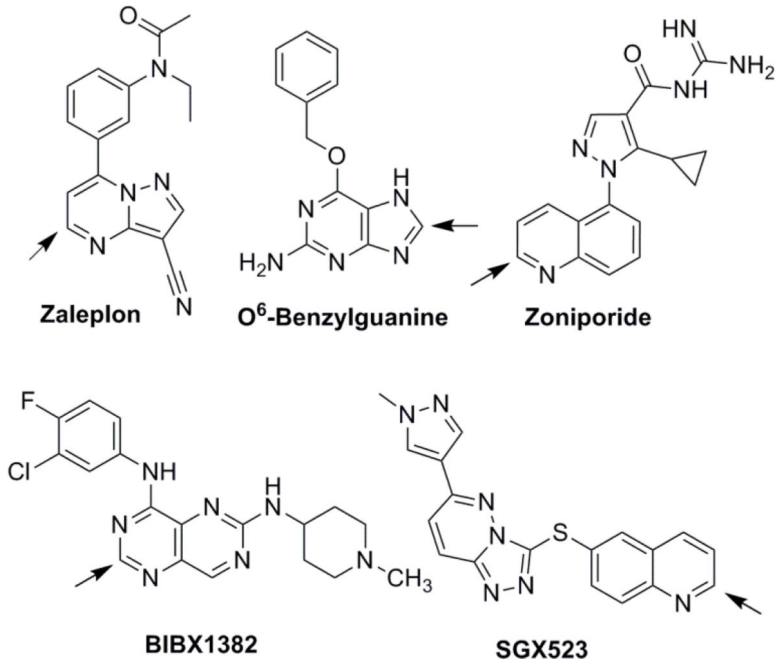

Figure 1.
Structures of AO substrates subjected to *in vitro* allometric scaling. Arrows indicate site of AO oxidation.

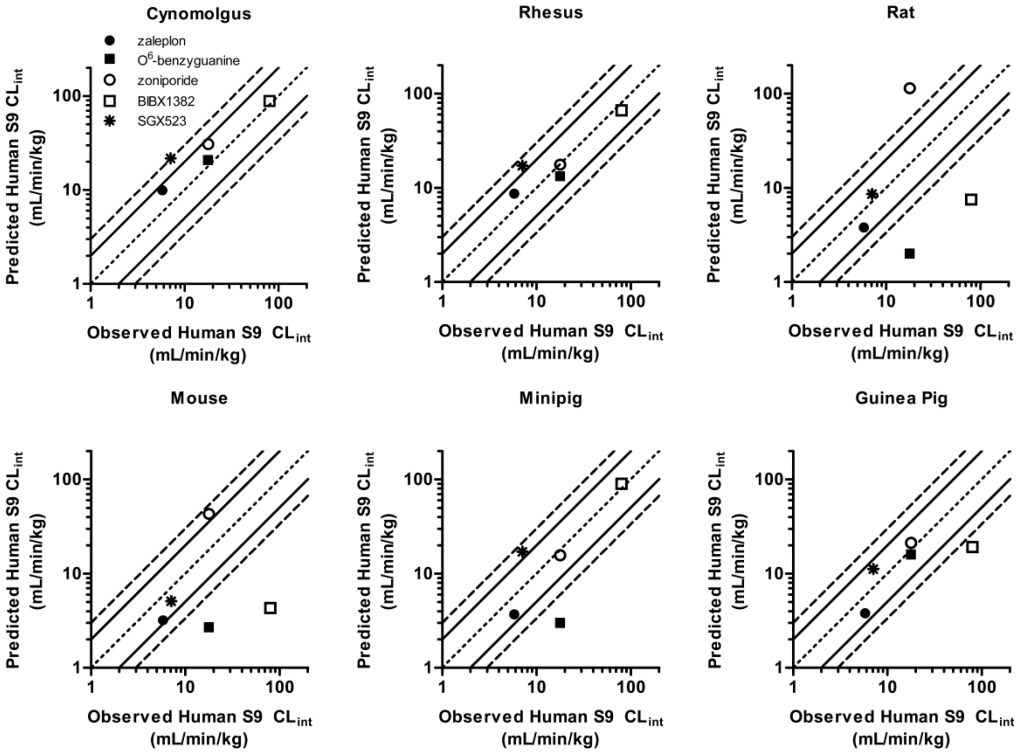

Figure 2.

Plots of observed human S9 CL_{int} vs that predicted from single-species scaling. Inner dotted line represents unity, solid line represents 2-fold-error, and outer dashed line represents 3fold-error. Zaleplon (•), O^6-benzylguanine (■), zoniporide (○), BIBX1382 (□), and SGX523 (*).

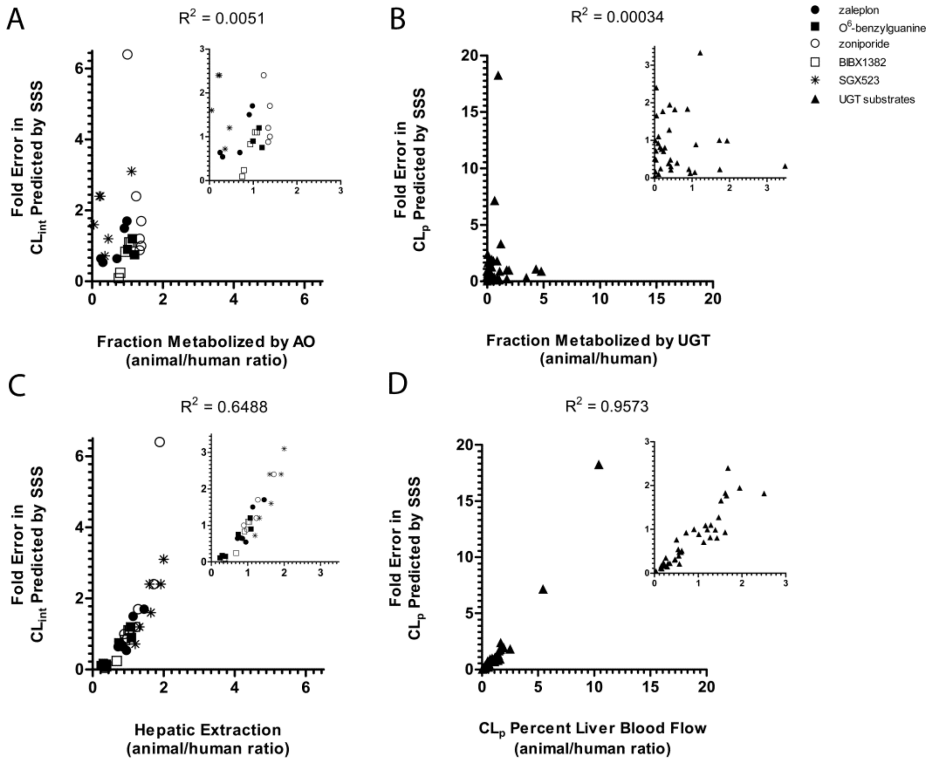

Figure 3.

Correlation of SSS fold-error and animal/human ratios of F_m E, or CL_p as a percentage of liver blood flow for *in vitro* data with AO substrates (**A** and **C**) or *in vivo* data with UGT substrates reported by Deguchi et al. (**B** and **D**). (**A**) fold-error in SSS of CL_{int} vs animal/human ratio of $F_{m,AO}$ (inset, axes magnified), (**B**) fold-error in SSS of CL_p vs animal/human ratio of $F_{m,UGT}$ (inset, axes magnified), (**C**) fold-error in SSS of CL_{int} vs animal/human ratio of E (inset, axes magnified), and (**D**) fold-error in SSS of CL_p vs animal/human ratio of CL_p as a percentage of liver blood flow (inset, axes magnified). Zaleplon (•), O^6-benzylguanine (■), zoniporide (○), BIBX1382 (□), and SGX523 (*). UGT substrates are collectively represented by (▲).

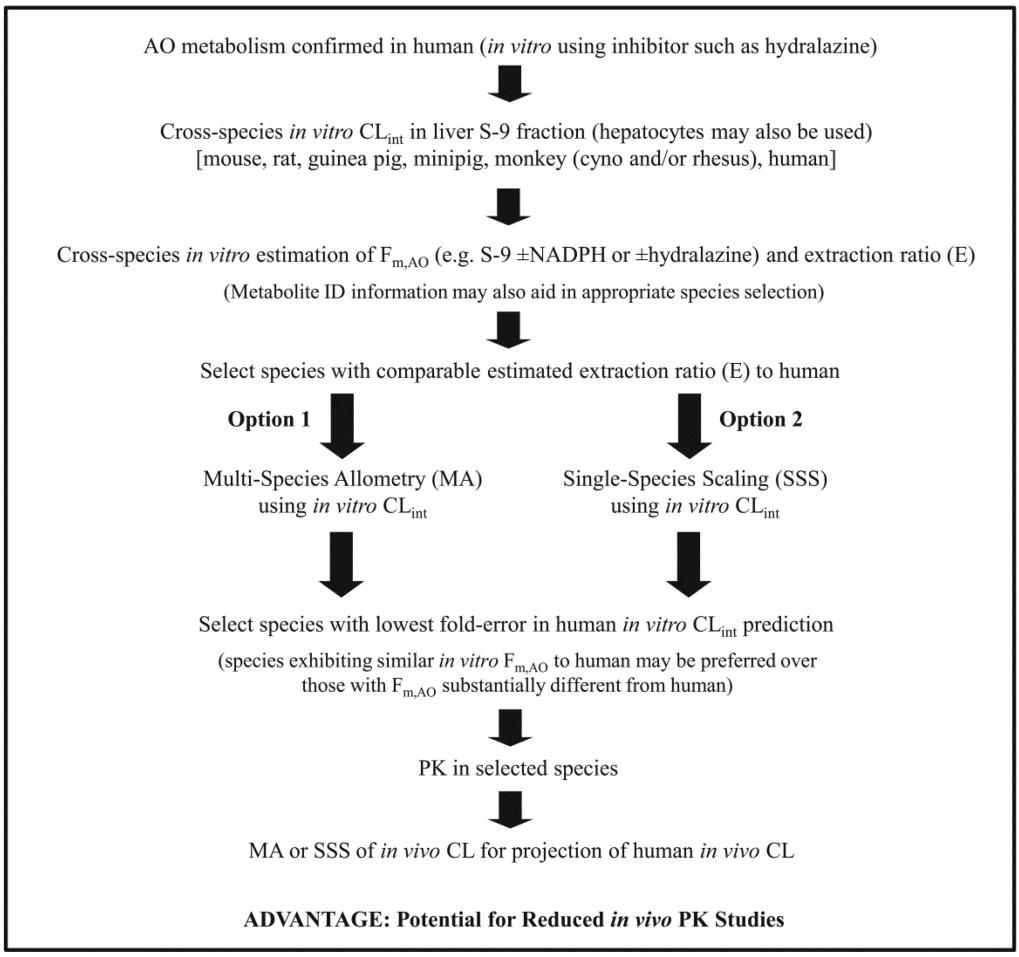

Figure 4.

Flow chart integrating current strategies to identify and predict human AO-mediated metabolism with a novel *in vitro* approach to guide selection of appropriate species to be employed in traditional (*in vivo*) allometric scaling for projection of human *in vivo* clearance.

Table 1.

Multispecies intrinsic clearance (CL_{int}, mL/min/kg) of zaleplon, O^6-benzylguanine, zoniporide, BIBX1382, and SGX523 in incubations with hepatic S9 (in the presence of NADPH).

	Zaleplon	O^6-benzylguanine	Zoniporide	BIBX1382	SGX523
Human	5.8 ± 1.02	17.8 ± 1.94	17.9 ± 1.77	80.2 ± 9.61	7.1 ± 2.28
Mouse	24.4 ± 5.28	20.7 ± 7.10	332 ± 11.3	33.2 ± 7.10	39.4 ± 7.19
Rat	15.6 ± 3.05	8.3 ± 2.03	466 ± 27.0	30.7 ± 3.56	35.3 ± 6.39
Guinea Pig	14.2 ± 1.89	60.3 ± 4.29	79.9 ± 7.47	72.7 ± 4.05	42.4 ± 4.71
Cynomolgus Monkey	20.3 ± 2.45	42.5 ± 8.40	62.8 ± 8.34	181 ± 11.5	44.4 ± 5.60
Rhesus Monkey	15.0 ± 2.06	22.9 ± 3.98	30.2 ± 3.29	114 ± 7.46	29.6 ± 7.22
Minipig	5.55 ± 1.34	4.43 ± 1.44	23.4 ± 2.07	134 ± 5.69	25.4 ± 1.46

Data represent means of triplicate determinations from 2–3 experiments (± SD).

Table 2.

Multispecies hepatic clearance (CL_{HEP}, mL/min/kg) of zaleplon, O^6-benzylguanine, zoniporide, BIBX1382, and SGX523 in incubations with hepatic S9 (in the presence of NADPH) and the estimated hepatic extraction ratio (E).

	Zaleplon		**O^6-benzylguanine**		**Zoniporide**		**BIBX1382**		**SGX523**	
	CL_{HEP}	E	CL_{HEP}	E	CL_{HEP}	E	CL_{HEP}	E	CL_{HEP}	E
Human	4.55 ± 0.625	0.22	9.62 ± 0.593	0.46	9.64 ± 0.503	0.46	16.6 ± 0.417	0.79	5.22 ± 1.15	0.25
Mouse	19.0 ± 3.35	0.21	16.6 ± 4.51	0.18	70.8 ± 0.517	0.79	24.1 ± 3.85	0.27	27.2 ± 3.66	0.30
Rat	12.7 ± 2.10	0.18	7.40 ± 1.61	0.11	60.8 ± 0.485	0.87	21.3 ± 1.73	0.30	23.3 ± 2.85	0.33
Guinea Pig	11.5 ± 1.25	0.19	30.3 ± 1.11	0.50	34.5 ± 1.40	0.57	33.1 ± 0.838	0.54	24.9 ± 1.64	0.41
Cynomolgus Monkey	13.9 ± 1.16	0.32	21.4 ± 2.28	0.49	25.8 ± 1.43	0.59	35.4 ± 0.434	0.80	22.0 ± 1.39	0.50
Rhesus Monkey	11.2 ± 1.14	0.25	15.0 ± 1.75	0.34	17.9 ± 1.16	0.41	31.7 ± 0.593	0.72	17.5 ± 2.69	0.40
Minipig	4.60 ± 0.934	0.16	3.79 ± 1.04	0.14	12.7 ± 0.620	0.45	23.1 ± 0.170	0.83	13.3 ± 0.401	0.48

Data, calculated using CL_{int} values from Table 1, represent means of triplicate determinations from 2–3 experiments (± SD).

Table 3.

Multispecies intrinsic clearance (CL_{int}) estimated from S9 fractions containing NADPH, containing NADPH and hydralazine, without NADPH, or containing hydralazine without NADPH, and the estimated fraction metabolized by AO ($F_{m,AO}$) calculated from the CL_{int} data using methods A and B.

Species	CL_{int} (mL/min/kg)				$F_{m,AO}$	
	+NADPH	+NADPH +Hyd	−NADPH	−NADPH +Hyd	Method A	Method B
Zaleplon						
Human	5.57 ± 1.01	n/c	3.96 ± 1.35	n/c	1	0.71
Mouse	28.0 ± 2.81	22.0 ± 6.14	n/c	n/c	0.22	0
Rat	18.0 ± 0.698	n/c	n/c	n/c	n/a	n/a
Guinea Pig	13.5 ± 1.90	n/c	6.73 ± 3.63	n/c	1	0.50
Cynomolgus Monkey	18.3 ± 1.41	n/c	12.8 ± 1.34	n/c	1	0.70
Rhesus Monkey	16.7 ± 1.31	9.61 ± 0.964	10.8 ± 0.743	n/c	0.42	0.65
Minipig	6.70 ±0.621	5.54 *	n/c	n/c	0.17	0
O^6-benzylguanine						
Human	17.8 ± 3.05	5.37 ± 1.16	14.8 ± 1.98	n/c	0.70	0.83
Mouse	15.5 ± 2.48	n/c	n/c	n/c	n/a	n/a
Rat	6.59 ± 0.664	n/c	n/c	n/c	n/a	n/a
Guinea Pig	58.7 ± 4.65	15.0 ± 2.14	48.7 ± 5.15	n/c	0.74	0.83
Cynomolgus Monkey	35.6 ± 5.10	n/c	33.5 ± 3.84	n/c	1	0.94
Rhesus Monkey	19.5 ± 2.05	n/c	21.3 ± 1.52	n/c	1	1 #
Minipig	4.68 ± 2.20	n/c	n/c	n/c	n/a	n/a
Zoniporide						
Human	17.0 ± 1.49	4.00 ± 0.442	17.1 ± 1.53	4.80 ±0.685	0.77	0.72
Mouse	331 ± 17.5	31.7 ± 1.12	297 ± 16.0	n/c	0.90	0.90
Rat	482 ± 13.9	125 ± 11.0	357 ± 25.1	9.70 ± 1.90	0.74	0.72
Guinea Pig	73.6 ± 2.61	11.6 ± 2.06	84.4 ± 2.75	12.9 ± 2.54	0.84	0.97
Cynomolgus Monkey	55.2 ± 1.73	5.74 ± 1.16	55.3 ± 1.63	n/c	0.90	1
Rhesus Monkey	27.8 ± 2.03	6.47 ± 3.97	31.2 ± 2.60	n/c	0.77	1 #
Minipig	22.1 ± 1.87	3.67 ± 1.55	21.5 ± 1.01	n/c	0.83	0.97
BIBX1382						
Human	71.6 ± 1.92	5.83 ± 1.22	69.6 ± 2.10	3.93 ± 1.75	0.92	0.92
Mouse	21.4 ± 10.9	n/c	n/c	n/c	n/a	n/a
Rat	27.6 ± 0.995	25.1 ± 6.29	19.0 ± 3.17	n/c	0.09	0.69
Guinea Pig	69.4 ± 1.66	24.5 ± 2.92	50.4 ± 1.13	n/c	0.65	0.73
Cynomolgus Monkey	172 ±1.26	n/c	209 ± 19.6	n/c	1	1 #
Rhesus Monkey	108 ± 5.43	6.03 ± 3.34	92.7 ± 1.21	n/c	0.94	0.86
Minipig	133 ± 6.98	20.0 ± 2.92	127 ± 7.08	n/c	0.85	0.96

Species	CL_{int} (mL/min/kg)				$F_{m,AO}$	
	+NADPH	+NADPH +Hyd	−NADPH	−NADPH +Hyd	Method A	Method B
SGX523						
Human	7.34 ± 3.34	4.70 ± 2.40	4.51 ± 0.310	n/c	0.36	0.61
Mouse	35.9 ± 10.3	24.2 ± 5.04	24.4 ± 9.31	16.5 ± 4.03	0.33	0.22
Rat	36.9 ± 4.23	21.4 ± 0.664	10.4 ± 3.20	n/c	0.42	0.28
Guinea Pig	38.2 ± 1.13	29.4 ± 3.05	15.8 ± 6.15	14.6 ± 6.05	0.23	0.03
Cynomolgus Monkey	39.4 ± 1.25	16.6 ± 3.42	26.9 ± 4.35	n/c	0.58	0.68
Rhesus Monkey	23.6 ± 4.13	15.6 ± 2.43	11.3 ± 0.942	7.97 ± 3.59	0.34	0.14
Minipig	26.0 ± 1.20	21.4 ± 1.98	3.20 ± 0.574	n/c	0.18	0.12

CL_{int} data represent means of triplicate determinations (±SD); $F_{m,AO}$ calculated using mean CL_{int} values

n/c = CL_{int} not calculated; mean ln[C] versus time slope not significantly different from zero

n/a = insufficient CL_{int} data to calculate $F_{m,AO}$

* mean of duplicate determinations

calculations resulting in an $F_{m,AO} > 1$ were assumed to be equal to 1

Table 4.

Average absolute fold-error (AAFE), average fold-error (AFE), and percentage of compounds predicted within 2 or 3 fold-error of observed CL_{int} measured in human S9, as predicted by single-species scaling.

Single species scaling	AAFE	AFE	% within 2 fold	% within 3 fold
Cynomolgus Monkey	1.6	1.6	80%	80%
Rhesus Monkey	1.4	1.2	80%	100%
Rat	4.1	0.56	40%	40%
Mouse	3.8	0.38	40%	60%
Minipig	2.0	0.76	60%	80%
Guinea Pig	1.7	0.76	80%	80%

Table 5.

Interspecies comparison of hepatic extraction ratio (E), fraction metabolized by AO ($F_{m,AO}$), and SSS predictions using *in vitro* CL_{int} (mL/min/kg) or *in vivo* CL_p (mL/min/kg) for zoniporide (top) and BIBX1382 (bottom).

Species	E*	$F_{m,AO}$#	S9 CL_{int}	SSS Human Predicted S9 CL_{int}	CL_p	SSS Human Predicted CL_p
Zoniporide						
Human	0.46	0.72–0.77	17.9	---	21§	---
Mouse	0.79	0.90	332	43.1	298§	39.2
Rat	0.87	0.72–0.74	466	114	237§	62.7
Cynomolgus Monkey	0.59	≥ 0.90	62.8	30.7	31§	15.2
BIBX1382						
Human	0.79	0.92	80.2	---	25–55¶	---
Mouse	0.27	n/a	33.2	4.3	55¶	7.2
Rat	0.30	≤ 0.69	30.7	7.5	55¶	13.4
Cynomolgus Monkey	0.80	1.0	181	88.7	118¶	56.0

*Data from Table 2

#Data from Table 3

§Obtained from: Dalvie D, Zhang C, Chen W, et al. (2010). Drug Metab Dispos 38:641–654.

¶Obtained from: Hutzler JM, Cerny MA, Yang YS et al. (2014). Drug Metab Dispos 42:1751–1760.

Table 6.

Human i.v. plasma clearance of zoniporide, O^6-benzylguanine, zaleplon, and BIBX1382 reported in the literature.

Compound	Human Plasma Clearance (mL/min/kg)
Zoniporide	21[*]
O^6-Benzylguanine	14.5[#]
Zaleplon	16[§]
BIBX1382	22–55[¶]
SGX523	N/A

[*] Dalvie D, Zhang C, Chen W, et al. (2010). Drug Metab Dispos 38:641–654.

[#] Dolan ME, Roy SK, Fasanmade AA, et al. (1998). J Clin Oncol 16:1803–1810.

[§] Rosen AS, Fournie P, Darwish M, et al. (1999). Biopharm Drug Dispos 20:171–175.

[¶] Dittrich C, Greim G, Borner M, et al. (2002). Eur J Cancer 38:1072–1080.